ELSEVIER

Journal of Hazardous Materials A67 (1999) 9–40

Journal of Hazardous Materials

Dispersion and thermodynamics of clouds generated from spills of SO_3 and oleum

T. Kapias *, R.F. Griffiths

Environmental Technology Centre, Department of Chemical Engineering, UMIST, PO Box 88, Manchester M60 1QD, UK

Received 5 November 1998; received in revised form 15 November 1998; accepted 26 January 1999

Abstract

A new model describing the dispersion behaviour and the processes that occur in a cloud generated from accidental spills of SO_3 and oleum has been developed. Such a cloud may initially behave as a dense gas, with several chemical and physical processes occurring in it. There is not usually enough atmospheric moisture in the air passing immediately above the pool for complete and rapid reaction to sulphuric acid mist. Therefore in the early stages, SO_3 vapour, H_2SO_4 vapour and H_2SO_4 aerosol will be present. At some distance downwind, transition to passive dispersion behaviour will take place and only sulphuric acid aerosol will be present in the cloud. The dense gas model is based on a box type dispersion model. The passive behaviour is described by a Gaussian model that takes into account deposition of the aerosol particles. The model results suggest a number of lines of experimental investigation that are required to provide data for model validation.

Keywords: SO_3; Oleum; Clouds

1. Introduction

SO_3 and oleums are highly reactive and aggressive materials that are used widely in the process industries. Their main feature is the rapid and highly exothermic reaction of SO_3 and water that occurs in both the liquid and the vapour phase. On escape to the environment they create liquid pools that can boil or evaporate or even solidify. The pool behaviour is governed by the amount of water available for reaction [1–3]. A detailed description of the model describing the pool behaviour can be found elsewhere

* Corresponding author. Tel.: +44-161-2003-855; Fax: +44-161-2003-988; E-mail: mjkmeztk@fs1.ce.umist.ac.uk

0304-3894/99/$ - see front matter
PII: S0304-3894(99)00015-1

[4]. Its main characteristic is that it describes the pool behaviour in a realistic way taking into account the numerous phenomena occurring in the pool. The same model could readily be used for pools created from spills of other reactive substances especially those with a strong affinity for water.

SO_3 and possibly H_2SO_4 (always in smaller amounts than SO_3 due to its much lower vapour pressure) will evolve from the pool. The evolution rates are higher for the pool spreading duration [1]. These vapours react with atmospheric moisture yielding sulphuric acid aerosol. SO_3 vapour, H_2SO_4 vapour and H_2SO_4 aerosol present a major hazard to humans and to the environment. The behaviour of the cloud (or plume) is very complicated as several interrelated physical and chemical processes are involved. The cloud initially behaves as a dense-gas cloud and only after some distance downwind will it become passive. Previous modelling attempts assumed that the cloud generated from pools of SO_3 or oleum behaves as a passive one that has reached its chemical end point almost instantaneously [5,6]. However it has been shown that there is not usually enough atmospheric moisture for complete and rapid reaction of SO_3 to H_2SO_4 aerosol [2,7,8].

A source window uptake model is used to calculate the vapour mass evolution rates and the cloud source temperature at the downwind edge of the pool [9]. Both SO_3 and H_2SO_4 vapour will start reacting with the atmospheric moisture in the entrained air yielding respectively H_2SO_4 vapour and H_2SO_4 aerosol. The utilisation of water vapour by the SO_3 vapour should be much higher than that used by H_2SO_4, in view of its higher affinity for water and because initially there is more SO_3 present. SO_3 vapour will also react heterogeneously and exothermically with the free liquid water that is present on the ground [10]. Therefore the ground surface temperature will vary with distance. H_2SO_4 vapour will also be deposited on the ground [11]. The dispersion model used, in its original form, does not allow for mass losses. Here, we have incorporated a mass depletion model to allow for deposition. The assumption is made that the mass loss is not sufficient to affect the validity of the dispersion model. This is substantiated by showing that the deposition mass fluxes are negligible compared to the other mass fluxes. However, the effect of this deposition is significant in respect of its influence on ground surface temperature. Although the cloud initial temperature may be quite high (Ref. [1] shows values of the pool temperature in the range 300 to 500 K), it will fall on dilution with air, although the processes that occur in the cloud are themselves either exothermic or thermoneutral. Therefore, the aerosol dew point will be reached within some small distance downwind, and the aerosol formed will condense [12,13]. At a certain distance all the SO_3 and H_2SO_4 vapour will be consumed, and only H_2SO_4 aerosol will be present; the cloud will continue to be dense until one of the transition criteria is satisfied. A transition model is used in order to estimate the transition from the final heavy gas characteristics to the initial passive ones [14,15]. From this point the aerosol concentration and the cloud characteristics are calculated by the partial reflection model which is a Gaussian based model that accounts for the aerosol deposition [16,17].

2. Heavy gas dispersion model

A simple approach has been adopted in order to calculate the cloud geometrical size, the distribution of chemical species concentration within the cloud etc., as a function of

downwind distance from the release point. It is based on a numerical box model and the cloud characteristics are estimated by a process of iteration by solving the lateral expansion velocity, mass continuity (top and edge air entrainment) and momentum continuity equations. A source window uptake model is used to describe and evaluate the vapour mass flow rates at the downwind edge of the pool [9]. It is assumed that the source evolution rate, temperature and radius are constant. It should be noted that although these properties are not actually constant during the evolution period, they are not highly variable for the pool spreading time [1]. The mean values are calculated by the pool model for the pool spreading time and they are used as input parameters in the source window uptake model.

2.1. Determination of the atmospheric stability class

There are numerous schemes for categorising atmospheric stability class. In this work two such schemes are required, namely that based on the standard deviation of horizontal wind direction σ_θ (used for determining dispersion coefficients), and the Monin–Obukhov length L (used in the particle deposition model) [9,18].

It should be noted that the description given in the following pages corresponds to continuous releases of SO_3 or oleum.

2.2. Source window uptake model

The vertical extent or depth of the source H_s (m) at the downwind edge of the pool is calculated by the following equation [9]:

$$H_s = H'_s + 2\sigma_{z,2R_p} \tag{1}$$

where $\sigma_{z,2R_p}$ is the vertical dispersion coefficient for distance equal to the pool diameter $2R_p$ (m) and H'_s (m) is the vertical extent or the source depth in the case of pure vapour flow [9]:

$$H'_s = \frac{M'}{\rho_v W_s U_{w,H'_s}} \tag{2}$$

where M' (kg s^{-1}) is the vapour mass release rate, U_{w,H'_s} (m s^{-1}) is the mean wind speed over a height H'_s, ρ_v (kg m^{-3}) is the vapour density and W_s (m) is the source width, which is equal to the pool diameter. The mean wind speed U_{w,H'_s} is calculated by using the logarithmic wind speed profile, and taking the mean value of the wind speed at 10 equally spaced linear intervals over the window height [9]. The vapour density is calculated by assuming that the perfect-gas law holds. The mass flow rate of air M'_{as} at the source window is given by [9]:

$$M'_{as} = \rho_a U_w W_s H_s \tag{3}$$

where ρ_a (kg m^{-3}) is the air density, and U_w (m s^{-1}) is the wind speed over a height H_s (calculated similarly to U_{w,H'_s}).

By calculating the air mass and by knowing the relative humidity, the amount of water available for reaction is calculated. A detailed description of the reactions and of the energy balance is given in Section 4. By performing the above calculations, the source height, depth, temperature and composition are found.

2.3. Dispersion model

The major assumptions governing the dispersion procedure are [9,16]:

- The mass flow rate of vapour through the source window is constant.
- Diffusion is negligible compared to advective transport in the longitudinal direction.
- Transport in the *longitudinal* direction due to gravitational effects is negligible compared to advective transport.
- The air entrainment rate is not affected by the presence of liquid aerosol particles.
- Dispersion of the cloud is modelled as a heavy gas "slab" moving downwind and diluting.

The lateral expansion velocity is given by [9,16]:

$$\frac{\mathrm{d}W}{\mathrm{d}x} = \frac{U_\mathrm{f}}{U_\mathrm{tr}} = \frac{k\sqrt{g\Delta' H}}{U_\mathrm{tr}} \tag{4}$$

where W (m) is the plume half-width, x (m) is the downwind distance from the source, U_f (m s^{-1}) is the radial spread velocity, U_tr (m s^{-1}) is the translational plume velocity, k is the Froude number, g (m s^{-2}) is the acceleration due to gravity, H (m) is the plume height and Δ' is the fractional density excess over air density given by [9,16]:

$$\Delta' = \frac{\rho_\mathrm{c}}{\rho_\mathrm{a}} - 1 \tag{5}$$

where ρ_c (kg m^{-3}) is the cloud density calculated by the perfect-gas law. The translational plume velocity U_tr is assumed to be the mean wind speed over the depth of the plume.

The mass continuity is given by the following equation [9,16]:

$$\frac{\mathrm{d}M'}{\mathrm{d}x} = M'_\mathrm{a} = 2\rho_\mathrm{a}(Wu_\mathrm{T} + Hu_\mathrm{E}) \tag{6}$$

where M'_a (kg s^{-1}) is the mass rate of entrainment of air per unit distance, M' (kg s^{-1}) is the mass rate of the cloud, u_T (m s^{-1}) is the top entrainment velocity, u_E (m s^{-1}) is the edge entrainment velocity given by [9]:

$$u_\mathrm{T} = \frac{u_1}{\sqrt{\dfrac{1}{\beta_2^2} + \dfrac{\mathrm{Ri}^2}{\beta_1^2}}} \tag{7}$$

where u_1 (m s^{-1}) is the longitudinal rms turbulent velocity of the air given by [9]:

$$u_1 = u^*(3.12 - 0.233\mathrm{SP}) \tag{8}$$

and u^* (m s^{-1}) is the friction velocity of the airflow which can be calculated by using the logarithmic wind speed profile provided the wind speed at a certain height and the surface roughness length z_o (m) are known. SP is the atmospheric stability parameter calculated by the following formula [9]:

$$\mathrm{SP} = 6.46 - 0.341\sigma_\theta + 0.0045\sigma_\theta^2 \tag{9}$$

The Richardson number Ri is given by the following equation [9]:

$$\mathrm{Ri} = \frac{g\Delta' L_1}{u_1^2} \tag{10}$$

where L_1 (m) is the turbulent length scale [19]:

$$L_1 = 1.776(H/H_r)^{0.48} H_r \tag{11}$$

in which H_r is a reference height usually taken to be equal to 10 m [18].

The edge entrainment velocity u_E is equal to [9]:

$$u_E = \alpha U_f \tag{12}$$

In Eqs. (7) and (12), α is the edge mixing coefficient $\approx (0.3–1.5)$, $\beta_1 \approx (0.05–0.13)$ and $\beta_2 \approx (0.1–0.5)$ are the first and second top mixing coefficients respectively. The selection of the values of these three coefficients depends on the circumstances [9,16,18]. The lateral expansion and the mass continuity equations are solved at small successive distance increments $\mathrm{d}x$ (m) and the plume width and mass of entrained air are calculated. By knowing the mass of entrained air and its relative humidity, the reactions that take place are described and an energy balance is conducted (Section 4.6) so that the plume composition and temperature are determined. At each distance increment all the above equations are solved by a process of iteration in order to determine the plume height.

2.4. Transition to passive behaviour

The criteria that are used in order to determine whether transition to passive behaviour has occurred are: $\mathrm{Ri} < 1$ or $\Delta' < 0.001$ [9]. The initial conditions of the passive phase are defined using continuity of the plume height H_t (m) and half-width W_t (m) at the transition point x_t (m) [14]. Following the widely used assumption that the cloud edges are defined by the 10% of peak concentration contour, the equivalent passive dispersion parameters, at the transition point (lateral and vertical standard deviations σ_{yt} and σ_{zt}) are [15]:

$$\sigma_{yt} = W_t/2.14, \tag{13}$$

$$\sigma_{zt} = H_t/2.14 \tag{14}$$

Not all plume parameters can be continuous at the transition point, since the Gaussian distribution has only two degrees of freedom [16]. In order to overcome this difficulty two methods can be used: the virtual source model [20] and the area source model [14]. In the present approach, the latter is used due to its simplicity. At distances downwind of

the transition point, the plume dispersion parameters are given by the following equations [14]:

$$\sigma_y^2(x) = \sigma_{yt}^2 + \sigma_y^2(x - x_t) = (W/2.14)^2 \tag{15}$$

$$\sigma_z^2(x) = \sigma_{zt}^2 + \sigma_z^2(x - x_t) = (H/2.14)^2 \tag{16}$$

The vertical and lateral standard deviations are calculated according to Hosker's scheme [21].

It should be noted that no aerosol deposition effects are taken into account in the dense gas regime although we include it in the passive regime, recognising the lack of data to validate the deposition model. It is assumed that this simplifying assumption is justifiable on the basis that the dense-gas regime is usually not very extensive.

3. Passive dispersion

3.1. Model

When transition to passive dispersion behaviour occurs, the cloud contains in most cases only H_2SO_4 aerosol (the conversion of SO_3 and H_2SO_4 to H_2SO_4 aerosol is usually complete before transition occurs). In order to account for the deposition effects on the cloud dispersion, the 'partial reflection model' approach has been adopted [17]. This model takes into account both gravitational settling and particle deposition. The formula that is used in order to calculate the aerosol concentration C (kg m^{-3}) is [17,18]:

$$C = \frac{M'_{\text{aerosol}}}{2\pi\sigma_z\sigma_y u}\exp\left(-\frac{y^2}{2\sigma_y^2}\right)\left\{\exp\left(-\frac{[z-h+(v_t x/u)]^2}{2\sigma_z^2}\right) + a(x_G)\exp\left(-\frac{[z+h-(v_t x/u)]^2}{2\sigma_z^2}\right)\right\} \tag{17}$$

where M'_{aerosol} (kg s^{-1}) is the mass rate of advection of the aerosol component, h (m) is the source height, y and z are the coordinates that refer to the lateral and vertical directions, respectively, u (m s^{-1}) is the wind speed at height z, v_t (m s^{-1}) is the average gravitational settling velocity and $a(x_G)$ is the reflection coefficient which can be computed by solving the following equations (using the trial and error method):

$$\left[h - \frac{v_t x_G}{u}\right]\frac{\sigma_z(x)}{\sigma_z(x_G)} = z + h - \frac{v_t x}{u} \tag{18}$$

$$a(x) = 1 - \frac{2v_d}{v_t + v_d + (uh - v_t x)\sigma_z^{-1}(d\sigma_z/dx)} \tag{19}$$

where v_d (m s^{-1}) is the average particle deposition velocity and $\sigma_z(x_G)$ is the vertical standard deviation calculated as in Eq. (16). The coefficient $a(x_G)$ is found by setting

the deposition equal to the difference between the fluxes from the real and image sources so that Eq. (19) is obtained. It should be noted that for gases or particles perfectly reflected at the ground the coefficient $a(x_G)$ is unity [17]. In the scenarios investigated here, the values of $a(x_G)$ are very close to unity as shown in Section 7.2.

It should be noted that in this model, the effective source height h is equal to the half height at the downwind pool edge. In other words it is assumed that the vapours are released from a point located at a height equal to the half height at the downwind pool edge.

3.2. Gravitational settling and particles deposition

Evidence from accidents and experiments suggests that H_2SO_4 aerosols are initially very small (particle radius 0.1–10 μm) [6,22]. Thus, the Stokes' law description (valid for particles with radii less than 10 to 30 μm) can be used to calculate the gravitational settling velocity v_t (m s^{-1}) of the aerosol particles:

$$v_t = \frac{2r^2 g \rho_p}{9\mu_a} \tag{20}$$

where ρ_p (kg m^{-3}) is the particle density, r (m) is the particle radius and μ_a is the dynamic viscosity of the medium ($\approx 1.8 \times 10^{-5}$ kg s^{-1} m^{-1} for air). The particle radii will increase with distance due to the aerosol growth. Unfortunately, there are no data on aerosol growth rates at high aerosol concentrations (see Section 4.4). It is assumed that no aerosol growth occurs and the particles will have a constant radius. A mean radius value is used assuming that larger particles will be formed at higher relative humidities. The following equation is used in order to estimate the particle radii:

$$r = \frac{f_w}{f_r} 10^{-6} \tag{21}$$

where f_w (kg of water/kg of total air) is the water vapour:air mass mixing ratio and f_r (m (kg of water/kg of total air)) is the value of f_w at which the particle mean radius would be equal to 1 μm. From accidents and experiments that have occurred in the past, it was shown that particles with a mean radius of 1 μm were observed at relative humidities of about 10% ($f_r \approx 0.001$). The above equation (for a relative humidity of 100%) will give us particles with mean radius of 10 μm ($f_w \approx 0.01$), which corresponds to the upper limit observed in accidents and experiments [6,22].

The dry deposition formula used is based on that in the EPA's revised ISC2 model that assumes that the dry deposition velocity v_d (m s^{-1}) is inversely proportional to the sum of the aerodynamic resistance r_a (m s^{-1}), the surface resistance r_s (m s^{-1}) and the transfer resistance r_t (m s^{-1}) [23,24]:

$$v_d = \frac{1}{r_a + r_s + r_t} \tag{22}$$

The aerodynamic resistance is given by [23,24]:

$$r_a = \frac{1}{0.4u^*}\left[\ln\left(\frac{z_d}{z_o}\right) - \Psi_H\left(\frac{z_d}{L}\right)\right] \tag{23}$$

where L (m) is the Monin–Obukhov length, z_d (m) is a reference height (assumed to be 10 m) and the function Ψ_H is given by [23,24]:

$$\begin{aligned} \Psi_H(z/L) &= -5z/L && \text{for } 0 < z/L \\ \Psi_H(z/L) &= 0 && \text{for } z/L = 0 \\ \Psi_H(z/L) &= 2\ln\left(\frac{1+(1-16z/L)^{1/2}}{2}\right) && \text{for } z/L < 0 \end{aligned} \tag{24}$$

The surface or laminar layer resistance is dependent on the Brownian diffusivity of the particles and can be estimated by the following equation [23,24]:

$$r_s = \left[\mathrm{Sc}^n + \frac{\mathrm{St}}{(1+\mathrm{St}^2)}\right]^{-1} u^{*-1} \tag{25}$$

where Sc is the Schmidt number given by [23,24]:

$$\mathrm{Sc} = \upsilon_a / D_B \tag{26}$$

where ν_a (m s^{-1}) is the kinematic viscosity of air ($\approx 1.5 \times 10^{-5}$ m^2 s^{-1}) and D_B (m^2 s^{-1}) is the Brownian diffusivity given by [23,24]:

$$D_B = 0.8 \times 10^{-9} \frac{T_a}{2r_p} \tag{27}$$

where T_a (K) is the air temperature.

The Stokes number St is given by [23,24]:

$$\mathrm{St} = \frac{\upsilon_t u^{*2}}{gn} \tag{28}$$

In Eqs. (25) and (28) n is a coefficient equal to [23,24]:
$n = -0.5$ for $z_o \leq 0.1$ m
$n = -0.7$ for $z_o > 0.1$ m
The transfer resistance is given by [23,24]:

$$r_t = r_a r_s \upsilon_t \tag{29}$$

4. Thermodynamic model

The thermodynamic model is independent of the dispersion model. The amount of atmospheric water available for reaction is calculated from the dispersion model and its value determines all the chemical processes and the temperature of the cloud.

4.1. Theory

Although there is much work in the literature on heavy gas dispersion models that include thermodynamic models for reactive chemicals, none of them is satisfactory in describing the processes that occur in a SO_3/H_2SO_4 cloud. These processes are shown in Fig. 1. The three stages involve the following processes.

First stage. Initially SO_3 vapour and (possibly) H_2SO_4 vapour will evolve from the pool and they will both react with atmospheric moisture generating H_2SO_4 aerosol. If the dew point is reached the aerosol will condense. During this stage SO_3 vapour, H_2SO_4 vapour and H_2SO_4 aerosol will be present and the cloud will be denser than air. For this period the processes that occur simultaneously are:

- SO_3 vapour reacts homogeneously with atmospheric water yielding H_2SO_4 vapour.
- SO_3 vapour reacts heterogeneously with water on the ground yielding H_2SO_4 liquid.
- H_2SO_4 vapour and water vapour nucleate to sulphuric acid aerosols (nucleation).
- H_2SO_4 vapour diffuses within the cloud and some is lost on the ground.

Second stage. At a certain point all the available SO_3 vapour and H_2SO_4 vapour will be consumed. At this stage only H_2SO_4 aerosol will be present and the cloud will still be denser than air. Losses of the aerosol by deposition on the ground are treated as being negligible in both the first and the second stage.

Third stage. After adequate dilution with air the cloud density will fall and transition to passive behaviour will occur. At this stage, aerosol deposition on the ground is estimated and included in the calculations (Eq. (17)).

It should be noted that in all three stages aerosol growth occurs. Unfortunately this process cannot currently be modelled for the conditions under investigation, as the

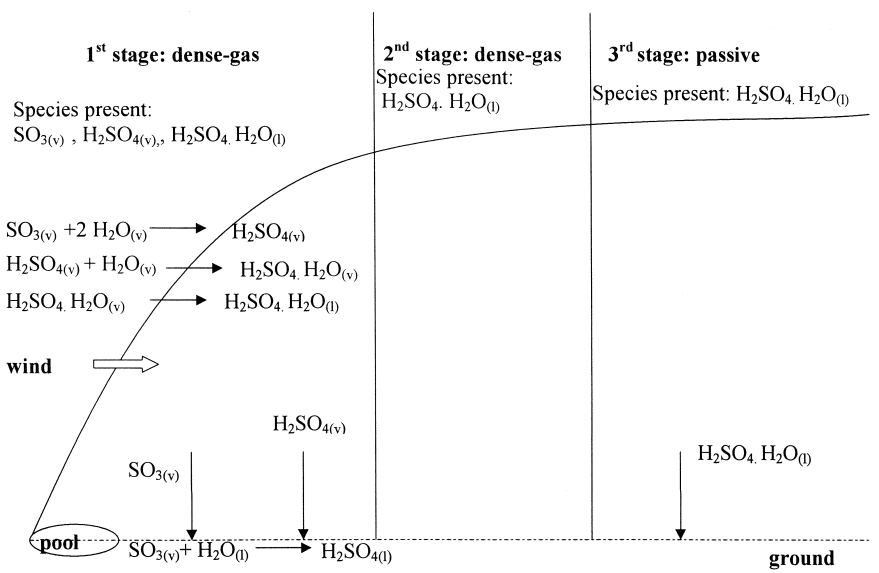

Fig. 1. Behaviour and processes that occur in a cloud generated from pools of SO_3 and oleum.

information available on this topic is restricted to concentrations corresponding to ambient atmospheric conditions, which are much lower than the levels of interest here.

4.2. Homogeneous reaction of SO_3 vapour and water vapour

The homogeneous reaction of SO_3 vapour with H_2O vapour has a long history of investigation. Even so, only very recently has it been found that the reaction mechanism involves one SO_3 and two H_2O molecules. Jayne et al. [10] have reported that the gas-phase reaction has a strong negative temperature dependence and no significant pressure dependence. The first-order rate coefficient for the SO_3 loss was reported to be equal to:

$$k_1 = 3.9 \times 10^{-41} \exp(6830.6/T)[H_2O]^2 \quad (s^{-1}) \tag{30}$$

where $[H_2O]$ is in units of molecule cm^{-3} and T is in Kelvin.

The observed loss of SO_3 due to the reaction with H_2O vapour can by represented by:

$$dSO_3/dt = -k_1[SO_3] \tag{31}$$

where $[SO_3]$ (molecule cm^{-3}) is the SO_3 concentration in the cloud.

The overall uncertainty of their experimentally determined rate coefficient was estimated to be $\pm 20\%$. At sufficiently low SO_3 concentrations ($< 10^{12}$ molecule cm^{-3} or $< 1.66\ 10^{-3}$ mg m^{-3}) the rate coefficient is independent of the initial SO_3 level. However, at higher concentrations and lower temperatures, increased loss rate coefficients were observed, indicating a fast heterogeneous reaction after the onset of binary homogeneous nucleation of acid hydrate clusters leading to particle formation. In the cloud under investigation here concentrations much higher than 1.66×10^{-3} mg m^{-3} are expected to be encountered especially in the very early stages. There is no clear indication of the SO_3 concentration below which Eqs. (30) and (31) can be applied. There is a clear possibility that these equations may estimate an SO_3 loss rate higher than its advective flux present in the cloud (especially in the very early stages, due to the much higher SO_3 concentrations encountered in the cloud compared to the ones experimentally investigated in Ref. [10]). In these cases all the available moisture will be consumed by the SO_3 and H_2SO_4 vapour in rapid reactions (see also Section 4.5).

4.3. Heterogeneous reaction of SO_3 with wet surfaces and H_2SO_4 vapour loss on the ground

The same authors also reported on the heterogeneous reaction of SO_3 with wet surfaces [10]. Because of the high SO_3 concentration in the cloud, this reaction will be diffusion limited. The SO_3–N_2 pressure-normalised gas-phase diffusion coefficient was reported to be equal to 94.6 (± 3) Torr $cm^2\ s^{-1}$ or 1.245 (± 0.004) 10^{-4} atm $m^2\ s^{-1}$ at 300 K. Some H_2SO_4 vapour will also be lost on the ground. The H_2SO_4–N_2 diffusion coefficient was reported to be 66.8 (± 1.1) Torr $cm^2\ s^{-1}$ or 0.8789 (± 0.0014) 10^{-4}

atm m^2 s^{-1} [11]. The diffusion-limited wall loss coefficient k_i (s^{-1}) in a tubular flow reactor can be approximated by [10,11]:

$$k_1 = \frac{3.66 D_p}{r^2 P} \tag{32}$$

D_p (Torr cm^2 s^{-1}) is the pressure-normalised gas-phase diffusion coefficient, r (cm) is the reactor radius and P (Torr) is the total pressure. The above equation has been extrapolated from the conditions of their experiments to the cloud conditions modelled here (their experiments were conducted at 300 K at a wide variety of pressure). If k_2 and k_3 (s^{-1}) are the SO_3 and H_2SO_4 coefficients respectively for the amount lost on the ground:

$$k_2 = \frac{11.4924 \times 94.6}{H \times 2W \times 10\,000 \times 760} \tag{33}$$

$$k_3 = \frac{11.4924 \times 66.8}{H \times 2W \times 10\,000 \times 760} \tag{34}$$

The respective loss rates due to the loss on the ground are [10,11]:

$$d[SO_3]/dt = -k_2[SO_3] \tag{35}$$

$$d[H_2SO_4]/dt = -k_3[H_2SO_4] \tag{36}$$

where $[H_2SO_4]$ (molecule cm^{-3}) is the H_2SO_4 concentration.

4.4. H_2SO_4 aerosol nucleation and growth

Unfortunately, all the theoretical and experimental data on H_2SO_4 aerosol nucleation and growth correspond to ambient atmospheric (or tropospheric and stratospheric) H_2SO_4 aerosol concentrations, which are extremely low compared to those of interest here. Furthermore, there is a large discrepancy between different theories and experimental results. For example, the H_2SO_4 mass accommodation coefficients are variously reported to be in the range 0.02–1 (the mass accommodation coefficient is defined as the probability with which a gas molecule colliding with a surface is incorporated into the liquid phase).

In order to describe aerosol nucleation the approach followed by Easter and Peters has been adopted [25]. Their formula has been modified by a factor of 10^{-6} to account for hydrate effects as indicated by the work of Jaecker-Voirol and Mirabel [26]:

$$J = \alpha' \times S_\alpha^{\beta'} \times 10^{-6} \ (\text{particles cm}^{-3}\ \text{s}^{-1}) \tag{37}$$

where α' and β' are constants dependent on the atmospheric relative humidity and S_α is the saturation ratio, given as a ratio of the acid pressure p_a, to its value over pure sulphuric acid p_{ae} [25]. The value for equilibrium pressure is given by the following equation [27]:

$$p_{ae} = 1.166 \times 10^{12} \exp(-10{,}156/T_c) \ (\text{N m}^{-2}) \tag{38}$$

It should be noted that the nucleation rate calculated from Eq. (37) is usually higher than the actual aerosol concentration would allow. Thus it is judged that the aerosol nucleation is a water availability limited process.

Although the cloud initial temperature may be high (depending on the source conditions), it will drop rapidly due to dilution with the surrounding air. The aerosol vapour phase will condense if the temperature drops to the dew point which is usually above 393 K (the aerosol dew point is reached within some very small distance downwind) [12,13]. The H_2SO_4 aerosol generated will grow, but unfortunately no existing model can describe this phenomenon when the aerosol mass concentration is higher than the atmospheric water mass concentration. In the model presented here a mean value for the particle radius is used and it is assumed that it remains constant. This value is proportional to the prevailing atmospheric relative humidity (see Section 3.2).

4.5. Mass balances

At each distance increment, the following mass balances for the first stage are conducted:

$$M'_{SO_3}(x_n) = M'_{SO_3}(x_{n-1}) - 0.5M'_{H_2O,1} - M'_{SO_3g} \quad (39)$$

$$M'_{H_2SO_4}(x_n) = M'_{H_2SO_4}(x_{n-1}) + 0.5M'_{H_2O,1} - M'_{H_2O,2} - M'_{H_2SO_4g} \quad (40)$$

$$M'_{aerosol}(x_n) = M'_{aerosol}(x_{n-1}) + M'_{H_2O,2} \quad (41)$$

$$M'_{air}(x_n) = M'_{air}(x_{n-1}) + M'_{\alpha}(x_n) - \left(M'_{H_2O,2} + 0.5M'_{H_2O,1}\right) \quad (42)$$

where $M'_{SO_3}(x_n)$ (kg s^{-1}) is the mass rate of advection of SO_3 vapour at the distance increment x_n and $M'_{SO_3}(x_{n-1})$ (kg s^{-1}) is the value at the previous distance increment, $M'_{H_2SO_4}(x_n)$ (kg s^{-1}) is the mass rate of advection of H_2SO_4 vapour at the increment x_n and $M'_{H_2SO_4}(x_{n-1})$ (kg s^{-1}) is the value at the previous distance increment, $M'_{aerosol}(x_n)$ (kg s^{-1}) is the mass rate of advection of H_2SO_4 aerosol at the distance increment x_n and $M'_{aerosol}(x_{n-1})$ (kg s^{-1}) is the value at the previous increment, $M'_{air}(x_n)$ (kg s^{-1}) is the mass rate of total air present at the distance increment x_n and $M'_{air}(x_{n-1})$ (kg s^{-1}) is its mass rate at the previous increment, $M'_a(x_n)$ (kg s^{-1}) is the mass rate of advection of the entrained air at x_n. $M'_{H_2O,1}$ (kg s^{-1}) is the mass rate of water consumed by the reaction of SO_3 vapour and $M'_{H_2O,2}$ (kg s^{-1}) is the mass rate of water consumed by the reaction of H_2SO_4 vapour. The total mass of water available at each distance increment is:

$$M'_{H_2O}(x_n) = M'_{H_2O}(x_{n-1}) + M'_{\alpha} f_1 \quad (43)$$

It should be noted that the $M'_{H_2O}(x_{n-1})$ represents the mass rate of water that is left in each increment due to the assumption that the reaction of SO_3 and water occurs on a 1:2 molecule basis.

As already mentioned in Section 4.2, there are two different cases depending on whether the calculated from Eqs. (30) and (31) SO_3 loss rate is higher than the advective flux of SO_3 present in the cloud. In other words, in some cases the first-order rate coefficient for the SO_3 loss calculated from Eq. (30) is much higher than the SO_3

concentration would allow and it is not suitable to be used in the SO_3 mass balance. In these cases all the atmospheric moisture is being consumed by the SO_3 and H_2SO_4 vapour and the reactions that occur are rapid.

The first case accounts for the balances when the calculated SO_3 loss rate is higher than the value present in the cloud. In these cases, the SO_3 loss becomes a water availability limited reaction. It is assumed that SO_3 has a 10 times greater affinity for H_2O than does H_2SO_4 vapour. The mass rates of water available for each reaction are calculated from the following equations:

$$\frac{M'_{H_2O,1}}{M'_{H_2O,2}} = 10\frac{M'_{SO_3}/80}{M'_{H_2SO_4}/98} \tag{44}$$

$$M'_{H_2O,1} + M'_{H_2O,2} = M'_{H_2O}(x_n) \tag{45}$$

In cases where the SO_3 loss rate is lower than the allowable value:

$$M'_{H_2O,2} = M'_{H_2O}(x_n) - M'_{H_2O,1} \tag{46}$$

and $M'_{H_2O,1}$ is calculated from Eqs. (30) and (31). The masses of SO_3 and H_2SO_4 that are lost on the ground are calculated by the following equations:

$$M'_{SO3g}(x_n) = M'_{SO3}(x_{n-1})k_2 t \tag{47}$$

$$M'_{H_2SO_4g}(x_n) = M'_{H_2SO_4}(x_{n-1})k_3 t \tag{48}$$

The term t (s) represents the time for the cloud to travel from x_{n-1} to x_n:

$$t = \mathrm{d}x/U_{tr} \tag{49}$$

In the second stage the mass rate of the aerosol is assumed to remain constant and in the third stage Eq. (17) accounts for the aerosol deposition on the ground.

4.6. Energy balance

An energy balance is conducted in each increment during the first and second stage, in order to calculate the cloud temperature. It takes into account all the reactions and processes that occur in the cloud, the enthalpies of all the components and the energy exchange of the cloud with the substrate. The reaction of SO_3 and water is highly exothermic and it provides the cloud with an amount of energy H_r (kJ) that equals [28,29]:

$$H_r = 102\,000 \times 0.5 M_{H_2O,1} \tag{50}$$

The nucleation of H_2SO_4 vapour to H_2SO_4 aerosol is a thermoneutral reaction. Energy is also being given to the cloud by the condensation of the aerosols. This energy H_{cond} (kJ) is calculated from the equation given below [12,29]:

$$H_{cond} = 71\,128 \times \frac{98}{18} M'_{H_2O,2} + 43\,932\, M'_{H_2O,2} \tag{51}$$

There will be an amount of energy consumed in order to bring the total mass of entrained air to the cloud temperature. This term consists of two parts, one for dry air and one for the water content [12,29]:

$$H_{\text{air}} = \left[\left(6.917\left(T_{\text{c}} - T_{\alpha}\right)\right) + \left(\left(0.00009911/2\right)\left(T_{\text{c}}^2 - T_{\alpha}^2\right)\right) + \left(\left(0.0000007627/3\right)\left(T_{\text{c}}^3 - T_{\alpha}^3\right)\right)\right] \times 4.184\left(M'_{\alpha}\left(1 - f_1\right)/28.8\right)$$

$$H_{\text{H}_2\text{O}} = \left[\left(7.17\left(T_{\text{c}} - T_{\alpha}\right)\right) + \left(\left(0.0256/2\right)\left(T_{\text{c}}^2 - T_{\alpha}^2\right)\right)\right] \times 4.184\left(M'_{\alpha} \times f_1/28.8\right) \quad (52)$$

where T_{c} (K) is the cloud temperature.

The enthalpy difference of the cloud components between successive steps, ΔH (kJ) is given by [12,28]:

$$\Delta H = \left\{\left[\left(z_{\text{SO}_3} \times 11.971\right) + \left(z_{\text{H}_2\text{SO}_4} \times 22.65\right) + \left(z_{\text{air}} \times 6.917\right) + \left(z_{\text{H}_2\text{O}} \times 7.17\right)\right]\left(T_c - T_{\text{c,pr}}\right) + \left[\left(\left(z_{\text{SO}_3} \times 0.006536\right) + \left(z_{\text{H}_2\text{SO}_4} \times 0.012562\right) + \left(z_{\text{air}} \times 0.00009911\right) + \left(z_{\text{H}_2\text{O}} \times 0.0256\right)\right)/2\right] \times \left(T_{\text{c}}^2 - T_{\text{c,pr}}^2\right) + \left[\left(\left(z_{\text{SO}_3} \times 0.0000001847\right) + \left(z_{\text{H}_2\text{SO}_4} \times 0.000003098\right) + \left(z_{\text{air}} \times 0.0000007627\right)\right)/3\right]\left(T_{\text{c}}^3 - T_{\text{c,pr}}^3\right)\right\} \times 4.184\left(M'_{\text{SO}_3}/80 + M'_{\text{H}_2\text{SO}_4}/98 + M'_{\text{air}}/28.8 + M'_{\text{H}_2\text{O}}/18\right) \quad (53)$$

where z_{i} (i = SO_3, H_2SO_4, air, H_2O) are the molecular fractions of the vapours in the cloud. It should be noted that due to the lack of precise thermodynamic data for the H_2SO_4 aerosol it has been assumed that its specific heat equals the specific heat of liquid H_2SO_4. The substrate temperature during the first stage will not be constant due to the exothermic heterogeneous reaction of SO_3 vapour with the free water lying on the ground yielding H_2SO_4 liquid. The ground surface temperature T_{g} (K) at each step is estimated by the following equation [12,29]:

$$\left(M'_{\text{SO}_3\text{g}}/80\right) \times 131\,035 = \left[\left(37.5\left(T_{\text{g}}\left(x_n\right) - T_{\text{g}}\left(x_{n-1}\right)\right) + \left(\left(0.006764/2\right) \times \left(\left(T_{\text{g}}^2\left(x_n\right) - T_{\text{g}}^2\left(x_{n-1}\right)\right)\right)\right)\right] 4.184 \quad (54)$$

where $T_{\text{g}}(x_n)$ (K) is the ground surface temperature at a distance increment x_n and $T_{\text{g}}(x_{n-1})$ (K) is the ground surface temperature during the previous increment. The heat transfer equation takes into account both the forced heat convection $H_{\text{g,f}}$ (kJ) and the natural heat convection $H_{\text{g,n}}$ (kJ). When $T_{\text{g}} < T_{\text{c}}$ this heat transfer consists only of that due to forced convection, while for $T_{\text{g}} > T_{\text{c}}$ the heat transfer is chosen to be the maximum of the forced and natural convection [30]. According to Witlox [30], who has rewritten the equation that Holman [31] derived for the forced convection heat transfer:

$$H_{\text{g,f}} = 1.22\left(u^{*2}/U_{10}\right)\rho_{\text{c}}C_{\text{pm}}U_{\text{tr}}\left(T_{\text{c}} - T_{\text{g}}\right)2WHt \quad (55)$$

where C_{pm} (kJ kg^{-1} K^{-1}) is the specific heat of the mixture, which is calculated by multiplying the molar fractions of the cloud components with their respective specific heats and then summing them. The natural convection heat is given by [29,32]:

$$H_{g,n} = \left\{0.14 g^{1/3}\left(P_a/R\right)\left[\left(\alpha_\tau/\nu\right)^2\left(\nu/T_c^2\right)\left(\mathrm{MW}_m C_{pm}\right)^3\right]^{1/3} \times \left[\left(T_g - T_c\right)^2/T_m\right]^{2/3}\right\} 2WHt \quad (56)$$

where P_α is the atmospheric pressure (1 atm), R is the gas constant, α_τ (m^2 s^{-1}) is the mixture thermal diffusivity, ν (m^2 s^{-1}) is the mixture kinematic viscosity, MW_m (kg kmol^{-1}) is the mixture molecular weight and T_m (K) is a mean temperature which is calculated from the following equation [30]:

$$T_m = \frac{T_c + T_g}{2} \quad (57)$$

The energy balance that is solved at each increment is given by the following equation:

$$H_r + H_{cond} = \Delta H + H_{air} + H_{H_2O} + H_{grd} \quad (58)$$

All the above equations are solved by the trial and error method in order to determine the cloud temperature T_c (K) in each step.

In the second stage no reactions take place ($H_r = H_{cond} = 0$) and the energy balance takes the following form:

$$\Delta H + H_{air} + H_{H_2O} + H_{grd} = 0 \quad (59)$$

5. Model calculations

The procedure that is followed to calculate all the cloud characteristics is complex, as follows. First, the pool model is run, in order to calculate the average pool radius and temperature and the mean vapour evolution rates for the spreading time. The atmospheric stability class is specified and all the atmospheric conditions are calculated (Section 2.1). Then the source window model is used in order to find the cloud characteristics at the downwind pool edge (Section 2.2). The heavy gas dispersion model (Section 2.3) in combination with the thermodynamic model (Section 4) are used for calculations in the first and second stages. When transition occurs, the transition model is used in order to determine the initial passive cloud characteristics (Section 2.4). Subsequently the passive cloud dispersion model is used (Section 3).

6. Model inputs and outputs

The inputs to the model are the σ_θ (standard deviation of the horizontal wind direction, degrees), the wind speed at a height of 10 m U_{10} (m s^{-1}), the roughness

length of the substrate z_o (m), the air temperature T_α (K), the air mass mixing ratio f_1 (kg of water vapour/kg of total air) or the relative humidity (%RH), the initial ground temperature T_{grd} (K), the free water film thickness on the ground w_g (m), the distance increment dx (m). The SO_3 and H_2SO_4 mean evolution rates M'_{SO_3} and $M'_{H_2SO_4}$ (kg s^{-1}), the mean pool radius R_p (m) and temperature T_p (K) are calculated by the pool model. The main outputs are the cloud width W (m) and height H (m), the mass rates of the substances in the cloud C_i (kg s^{-1}), the cloud temperature T_c (K), the cloud density ρ_c (kg m^{-3}) and the Richardson number Ri (for the first and second stage), as functions of the distance from the source x (m).

7. Results and conclusions

A number of different release scenarios have been investigated in order to examine the cloud behaviour. First, the pool model was run, to estimate the mean values of the pool temperature and radius and the vapour evolution rates. It should be noted that these values (except for scenario 9) correspond to the pool spreading time. It was shown that for this time, the observed evolution rates are much higher compared to the ones after spreading ceases. Therefore it was judged to be more appropriate (for risk analysis purposes) to present mainly the results corresponding to the pool spreading duration. The hazardous chemicals concentrations observed for the time after spreading ceases are much lower [4]. The results shown below are a representative sample from a large number of runs. The input parameters that correspond to the scenarios under investigation are shown in Table 1. The influence of the source strength (type of spill), the relative humidity and the wind speed have been examined.

Table 1
Input parameters for scenarios under investigation

Scenario	Spill type	w_g (m)	f_1 (kg of water (kg of total air)$^{-1}$) (RH)	R_p (m)	T_p (K)	M'_{SO_3} (kg s^{-1})	$M'_{H_2SO_4}$ (kg s^{-1})	U_{10} (m s^{-1})
1	20% oleum	0.001	0.005 (50%)	8.556	417.84	0.230	0.003	5
2	30% oleum	0.001	0.005 (50%)	8.39	442.43	0.808	0.010	5
3	65% oleum	0.0005	0.005 (50%)	7.91	343.75	1.604	0	5
4	65% oleum	0.001	0.001 (10%)	7.39	386.92	3.358	0.0003	5
5	65% oleum	0.001	0.005 (50%)	7.39	387.55	3.371	0.0003	5
6	65% oleum	0.001	0.01 (100%)	7.39	389.01	3.389	0.0003	5
7	65% oleum	0.002	0.005 (50%)	7.268	476.28	4.448	0.115	5
8	SO_3	0.001	0.005 (50%)	6.246	325.68	5.904	0	5
9[a]	65% oleum	0.001	0.005 (50%)	11.54	301.1	0.176	0	5
10	65% oleum	0.001	0.005 (50%)	7.39	387.55	3.371	0.0003	2
11	65% oleum	0.001	0.005 (50%)	7.39	387.55	3.371	0.0003	8
12[b]	65% oleum	0.001	0.005 (50%)	7.39	387.55	3.371	0.0003	5
13[c]	65% oleum	0.001	0.005 (50%)	7.39	387.55	3.371	0.0003	5
14[d]	65% oleum	0.001	0.005 (50%)	7.39	387.55	3.371	0.0003	5

[a] Scenario 9 corresponds to the time after spreading ceases.
[b] In scenario 12, the affinity of SO_3 vapour for water is equal to the affinity of H_2SO_4.
[c] In scenario 13, SO_3 has 5 times greater affinity for moisture than H_2SO_4 has.
[d] In scenario 14, SO_3 has 20 times greater affinity for moisture than H_2SO_4 has.

As already mentioned it has been assumed that SO_3 vapour has a 10 times greater affinity for moisture than has H_2SO_4 vapour (in cases where the available formulas for the calculation of the vapour loss rates give higher results than the actual concentrations would allow (see Section 4.5)). The effect of this assumption on the results has also been examined.

All the scenarios in Table 1 correspond to continuous releases of 16 kg s^{-1} for 600 s. The rest of the input parameters have the same values for all the scenarios and are equal to: $\sigma_\theta = 10°$, $dx = 0.01$ m, $U_{10} = 5$ m s^{-1}, $z_o = 0.1$ m, $T_\alpha = 288$ K and $T_{grd} = 283$ K. The entrainment coefficients chosen were: $\alpha = 0.7$, $\beta_1 = 0.08$ and $\beta_2 = 0.3$. The new model has been implemented in a computer programme in Microsoft Visual Basic Professional Edition 5.0. The cloud behaviour is investigated separately in the two regimes (heavy and passive gas behaviour).

7.1. Heavy gas regime (first and second stage)

In these stages, the cloud is denser than air and in the first stage SO_3 vapour, H_2SO_4 vapour and H_2SO_4 aerosol are present in the cloud. All the chemical processes occur during this stage. In the second stage only H_2SO_4 aerosol is present and no physical or chemical interactions take place. The parameters that mostly affect the cloud behaviour are the atmospheric conditions (especially the wind speed and the atmospheric humidity) and the source strength (vapour evolution rates from the pool).

Even for spills of low strengths (spills of 20% or 30% oleum) there is not usually enough atmospheric moisture for complete and rapid reaction of SO_3 to H_2SO_4 vapour (Fig. 2). Only when the relative humidity is very high (e.g. 100%, Scenario 6), is there enough atmospheric moisture above the pool for rapid reaction of SO_3 vapour to H_2SO_4 vapour. Even so, the cloud will initially contain H_2SO_4 vapour and H_2SO_4 aerosol and it will still be denser than air.

The higher the relative humidity (or the air mass mixing ratio) and lower the source strength, the lower are the lifetimes of SO_3 and H_2SO_4 in the cloud (Figs. 2 and 3). The higher the wind speed is, the lower (usually) the lifetimes of the species are and the faster transition to passive behaviour occurs (Fig. 4).

The calculated Richardson numbers for relatively high values of the wind speed (e.g., $U_{10} = 5$ m s^{-1} or 8 m s^{-1}) are not extremely high (Figs. 5–7), indicating that the cloud will not be very dense. For lower values of wind speed ($U_{10} = 2$ m s^{-1}) the calculated Richardson numbers are much higher, indicating that the lower the wind speed is, the denser the cloud is (Fig. 8).The higher the relative humidity and the source strength (defined by either the spill type or the free ground water film thickness), the higher the Richardson number is (Figs. 5–7). In all these figures the downwind pool edge is shown. The Richardson number generally decreases with increasing wind speed (Fig. 8). In most of the investigated cases the criterion that was first reached for transition to passive behaviour was $Ri < 1$ (except for scenario 10). Transition occurred in the range 50 to 450 m in these scenarios. The duration of the second stage is usually shorter than the first stage. In this stage due to dilution with air, the cloud density drops and transition to passive behaviour occurs. The plume height and width for this regime is

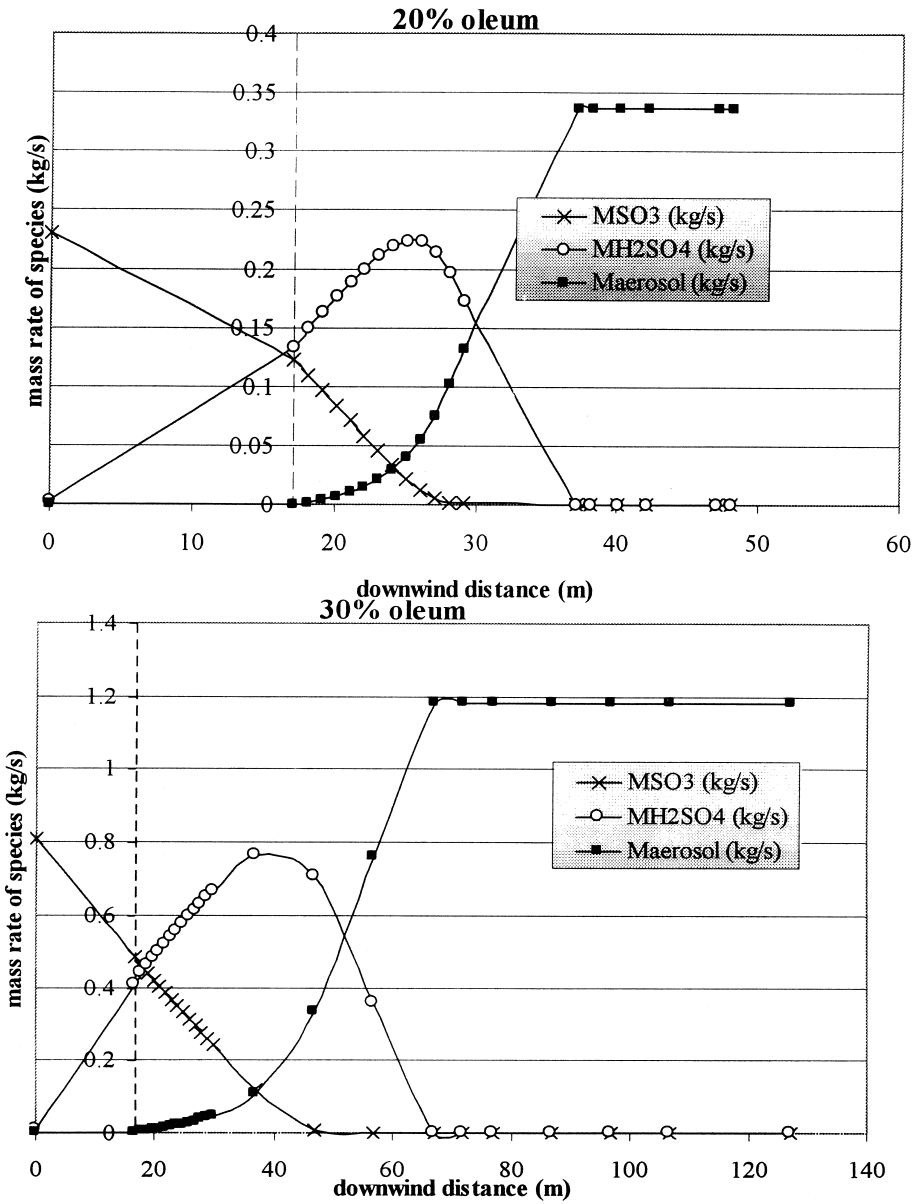

Fig. 2. Cloud composition for scenarios 1 and 2 (the dashed lines indicate the downwind pool edge).

given in Fig. 9. The cloud height increases with decreasing relative humidity due to the lower cloud density values observed at lower values of relative humidity. The cloud width usually increases with increasing values of relative humidity. The total species concentration (SO_3 vapour, H_2SO_4 vapour and H_2SO_4 aerosol) usually increases with

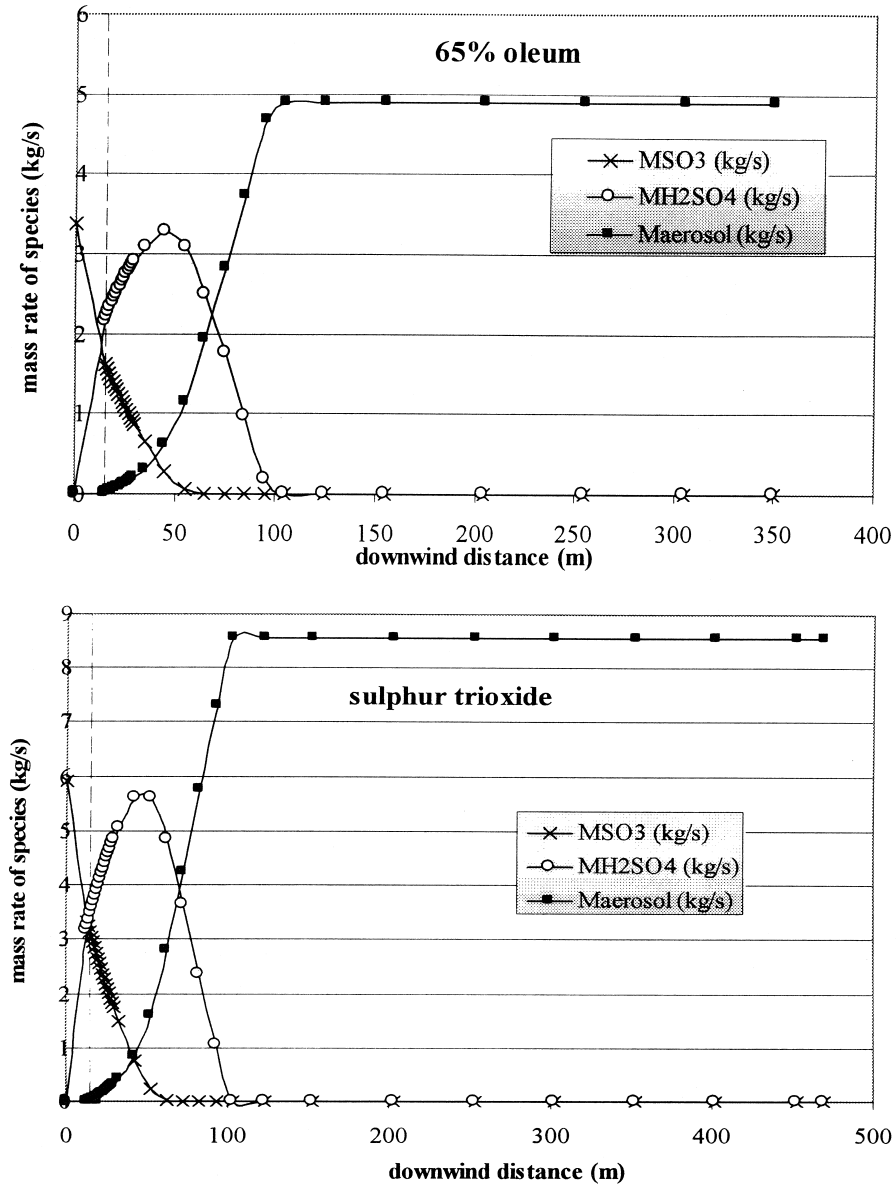

Fig. 3. Cloud composition for scenarios 5 and 8 (the dashed lines indicate the downwind pool edge).

increasing values of relative humidity (Fig. 10) and with increasing wind speed (Fig. 11). The amounts of SO_3 and H_2SO_4 lost on the ground are always much lower than 1% of the total mass released to the air. Generally the wind speed effect on the cloud behaviour is stronger than the relative humidity or the source strength effect.

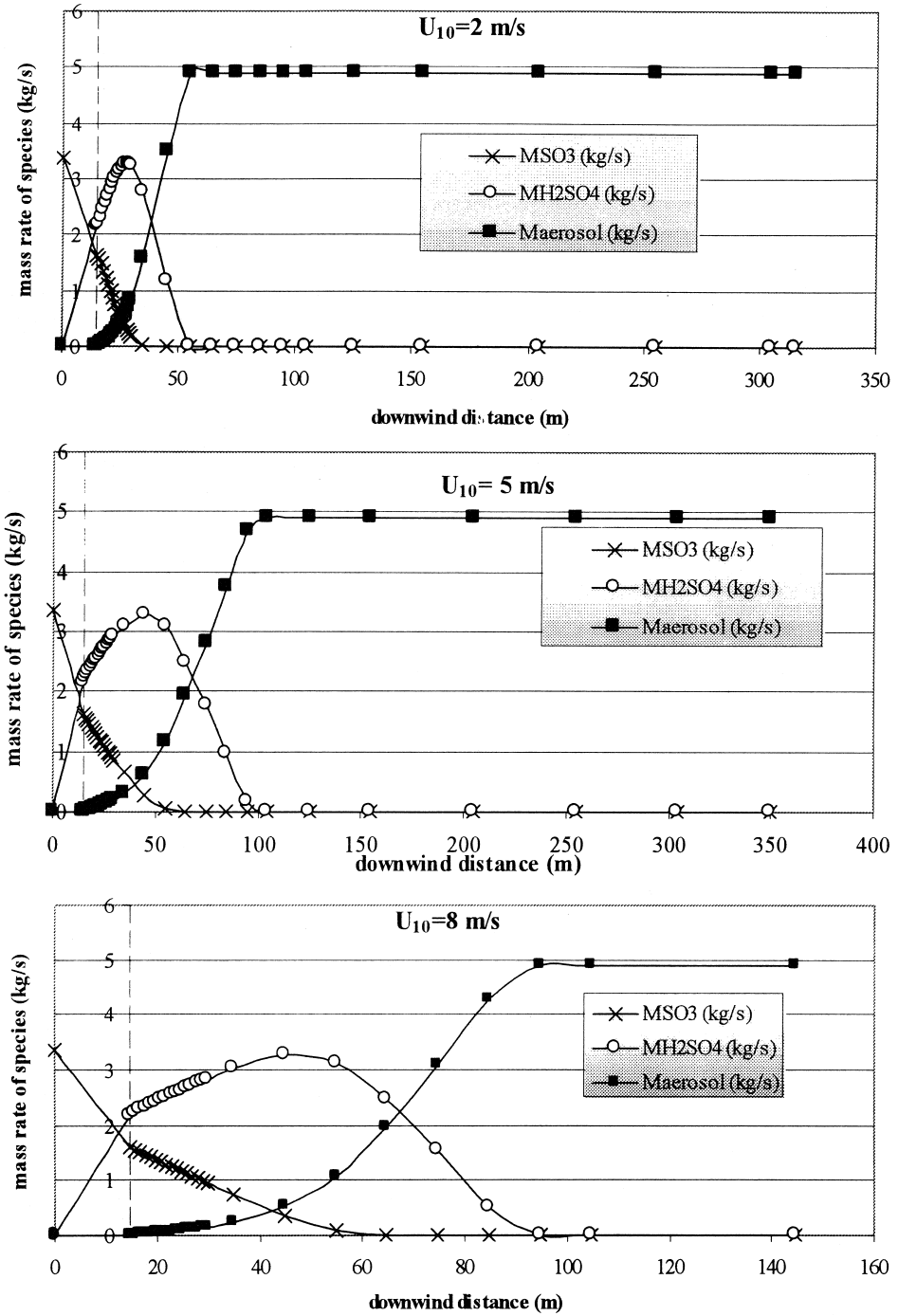

Fig. 4. Cloud compositions for scenarios 5, 10, 11 (wind speed effect) (the dashed lines indicate the downwind pool edge).

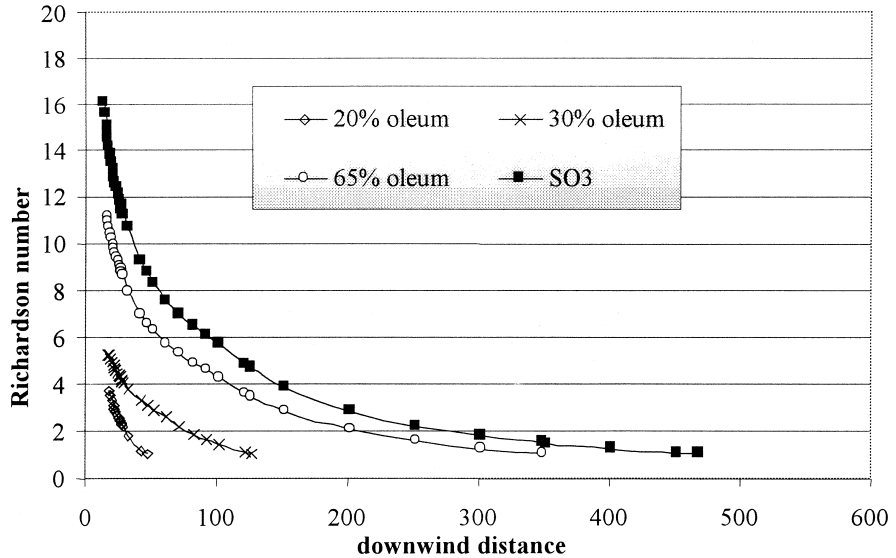

Fig. 5. Richardson number for scenarios 1, 2, 5 and 8 (spill type (or strength) effect).

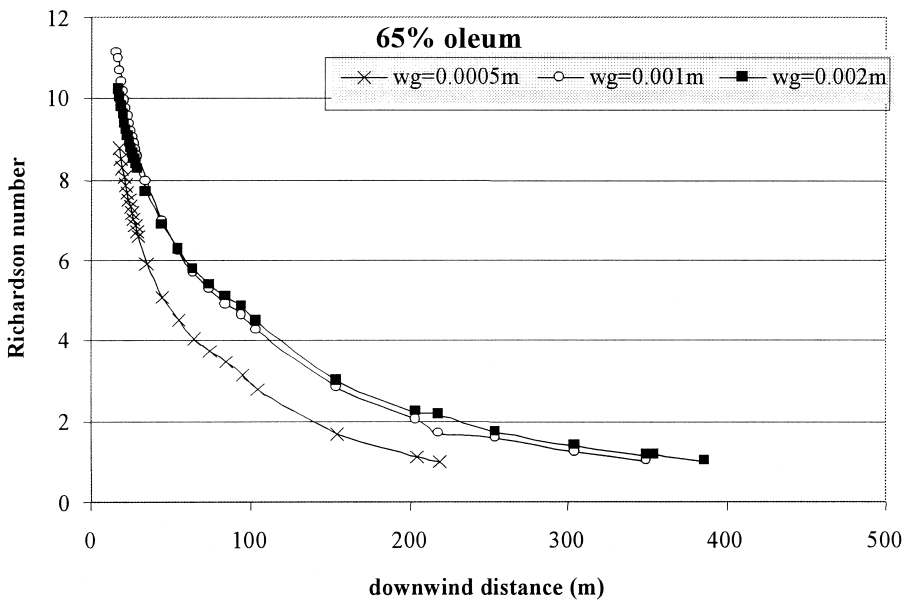

Fig. 6. Richardson number for scenarios 3, 5 and 7 (free ground water film thickness effect).

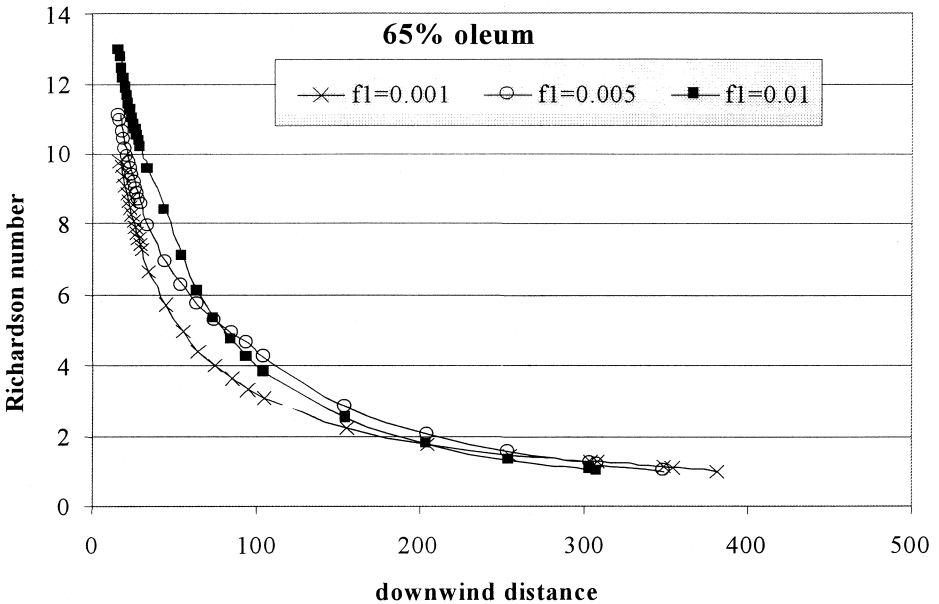

Fig. 7. Richardson number for scenarios 4, 5 and 6 (relative humidity effect).

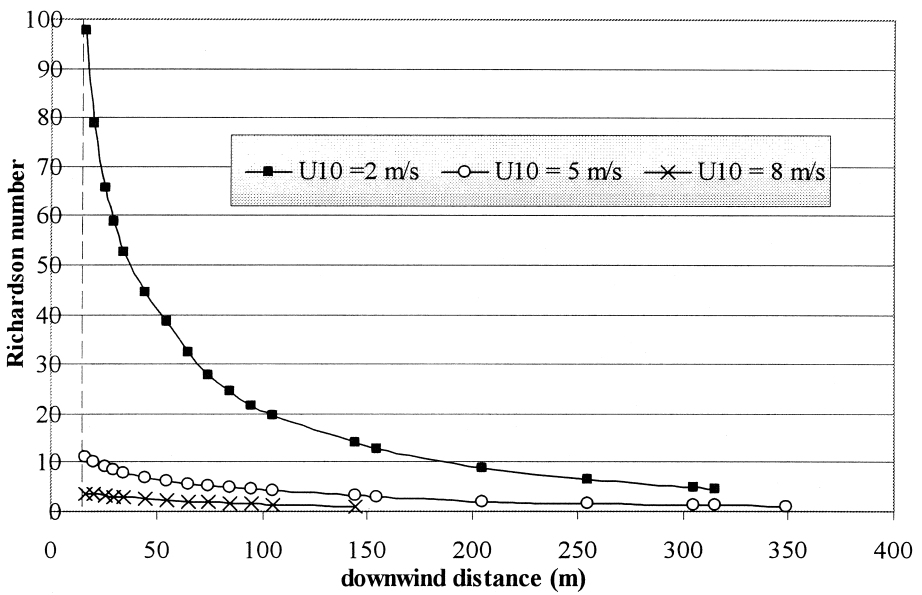

Fig. 8. Richardson number for scenarios 5, 10 and 11 (wind speed effect) (the dashed line indicates the downwind pool edge).

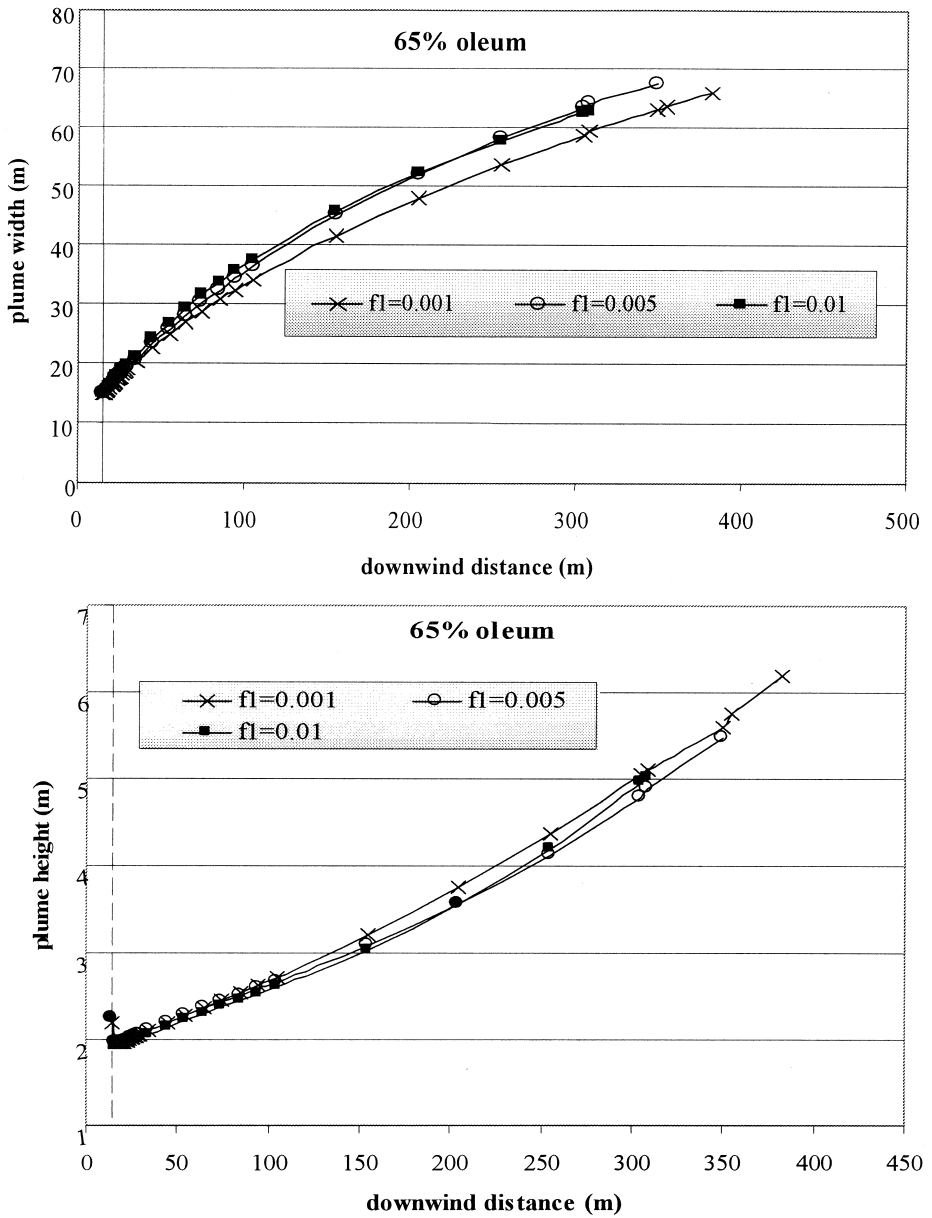

Fig. 9. Plume width and height for scenarios 4, 5 and 6 (relative humidity effect) (the dashed lines indicate the downwind pool edge).

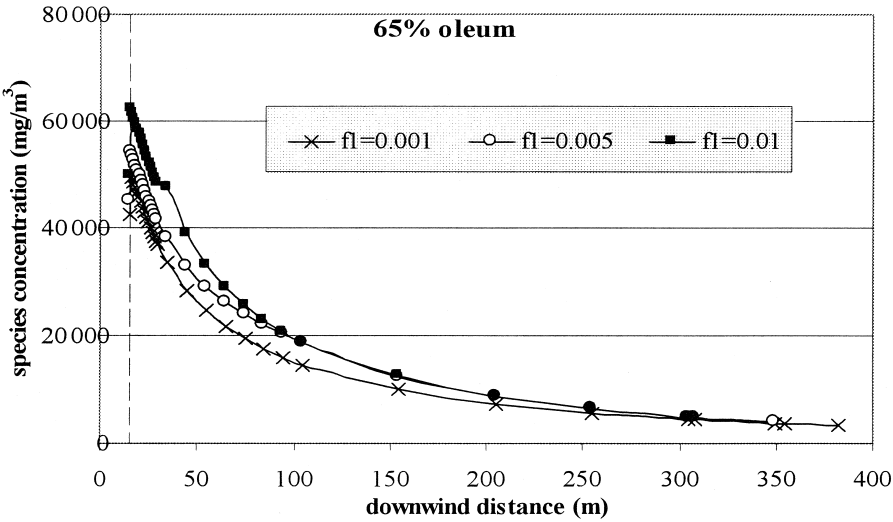

Fig. 10. Special total concentration for scenarios 4, 5 and 6 (relative effect) (the dashed lines indicates the downwind pool edge).

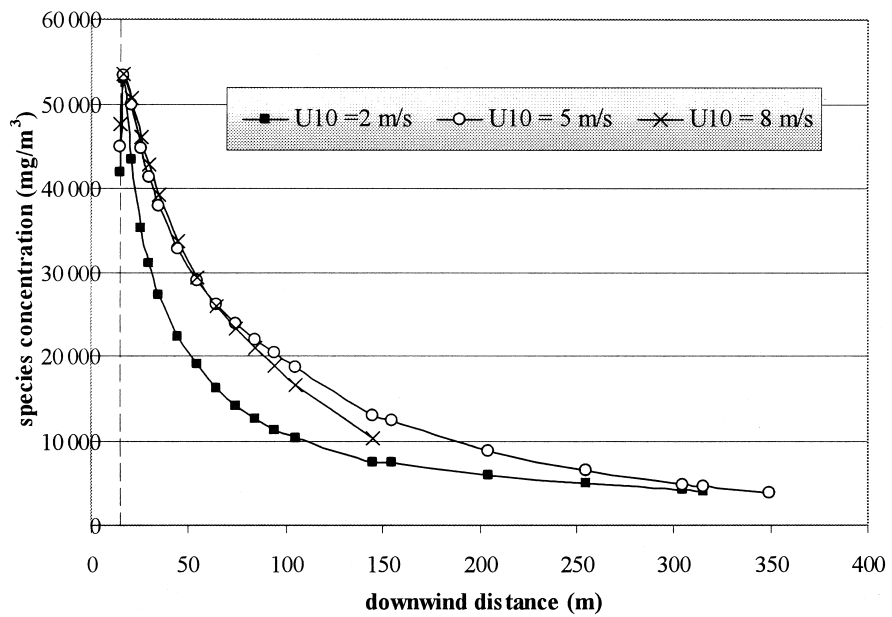

Fig. 11. Special total concentration for scenarios 5, 10 and 11 (wind speed effect) (the dashed lines indicates the downwind pool edge).

7.2. Passive behaviour regime (third stage)

In this regime, only H_2SO_4 aerosol is present in the cloud. Some is lost on the ground due to gravitational settling and deposition. The cloud behaviour in this stage is governed by the atmospheric conditions and especially by the value of the prevailing atmospheric humidity and the wind speed which determines the particle sizes and thus their settling and deposition velocities.

The centreline aerosol concentration for six different release scenarios is given in Tables 2 and 3. The average settling velocity (v_t), the deposition velocities (v_d) and the partial reflection factor $a(x_G)$ are also given in these tables.

Although in the dense gas regime, higher concentrations corresponded to higher values of relative humidity (Fig. 10) and higher values of wind speed (Fig. 11), in the passive regime it is the opposite. The higher the relative humidity, the lower the centreline aerosol concentration is (especially within small distances downwind (e.g., < 2000 m), because higher values of relative humidities will create larger particles with much higher settling velocities as shown in Table 2. The aerosol centreline concentration decreases with increasing wind speed for the same reason.

The reflection factor $a(x_G)$ takes values close to unity (usually around 0.95) for almost all the release scenarios indicating that the majority of the generated particles are not deposited. It has been found that for these values of the reflection factor, the particles deposition fraction is less than 5% of the total aerosol mass.

7.3. Behaviour of the cloud for the time after pool spreading ceases

Results from the pool model indicate that the vapour evolution rates are much lower for the time after pool spreading ceases, compared to the ones corresponding to the pool spreading duration. For the pool spreading time, the pool encounters free water lying on the ground (which is usually the dominant water source) and hence the amount of water available for reaction is higher [4].

After investigating a large number of releases for the time after pool spreading ceases, it has been found that transition to passive behaviour in this regime occurs rapidly and within some small distance downwind (typically < 50 m), and the estimated aerosol centreline concentration is much lower than that during pool spreading. For spills of 65% oleum ($w_g = 0.001$ m and RH $\approx 50\%$) for a duration of 600 s the results for the time after spreading ceases (scenario 9) and before spreading ceases (scenario 5) are shown in Table 4. It is assumed that emergency intervention takes place at 1800 s, terminating the vapour evolution.

7.4. Model sensitivity to the assumption concerning the SO_3 and H_2SO_4 affinity for moisture

The sensitivity of the model to the assumption that SO_3 vapour has 10 times greater affinity for moisture than H_2SO_4 vapour has been examined. It has been found that the model results are not sensitive to this assumption, as shown in Table 5.

Table 2
Centreline aerosol concentration at different values of relative humidity (Scenarios 4, 5 and 6)

Downwind distance (m)	Aerosol concentration (mg m^{-3}), Scenario 4, RH ≈ 10%	Aerosol concentration (mg m^{-3}), Scenario 5 RH ≈ 50%	Aerosol concentration (mg m^{-3}), Scenario 6 RH ≈ 100%
308.37[a]			4596
349.41[a]		3793	
391.86[a]	3284		
500	164.9	118.4	72.5
1000	10.88	9.60	8.35
2000	1.81	1.73	1.65
3000	0.770	0.755	0.731
4000	0.444	0.437	0.430
5000	0.297	0.295	0.291
6000	0.218	0.216	0.214
7000	0.169	0.168	0.167
8000	0.137	0.136	0.136
9000	0.114	0.114	0.113
10,000	0.097	0.097	0.097
v_t (cm s^{-1})	0.022	0.557	2.228
v_d (cm s^{-1})	0.729	0.725	0.713
$a(x_G)$[b]	0.949	0.952	0.959

[a]At these distances transition to passive behaviour occurs.
[b]Average value.

Table 3
Centreline aerosol concentration at different values of wind speed (Scenarios 5, 11 and 12)

Downwind distance (m)	Aerosol concentration (mg m^{-3}), Scenario 10 $U_{10} = 2$ m s^{-1}	Aerosol concentration (mg m^{-3}), Scenario 5 $U_{10} = 5$ m s^{-1}	Aerosol concentration (mg m^{-3}), Scenario 11 $U_{10} = 8$ m s^{-1}
144.57[a]			10,334
315.32[a]	4070		
349.41[a]		3793	
500	119.4	118.4	21.3
1000	19.19	9.60	3.76
2000	4.06	1.73	0.890
3000	1.82	0.755	0.417
4000	1.07	0.437	0.252
5000	0.726	0.295	0.173
6000	0.536	0.216	0.129
7000	0.418	0.168	0.101
8000	0.339	0.136	0.083
9000	0.284	0.114	0.069
10 000	0.243	0.097	0.057
v_t (cm s^{-1})	0.557	0.557	0.557
v_d (cm s^{-1})	0.290	0.725	1.160
$a(x_G)$[b]	0.971	0.952	0.962

[a]At these distances transition to passive behaviour occurs.
[b]Average value.

Table 4
Centreline aerosol concentration for scenarios 5 and 9

Downwind distance (m)	Aerosol concentration (mg m^{-3}), Scenario 9	Aerosol concentration (mg m^{-3}), Scenario 5
23.09[a]	0.176	
349.41[a]		3793
1000	140×10^{-6}	9.88
2000	40×10^{-6}	1.77
3000	20×10^{-6}	0.769
4000	10×10^{-6}	0.447
5000	8×10^{-6}	0.301
6000	6×10^{-6}	0.221
7000	5×10^{-6}	0.171
8000	4×10^{-6}	0.139
9000	3×10^{-6}	0.116
10 000	3×10^{-6}	0.099
v_t (cm s^{-1})	0.557	0.557
v_d (cm s^{-1})	0.725	0.725
$a(x_G)$[b]	0.971	0.952

[a]At these distances transition to passive behaviour occurs.
[b]Average value.

7.5. Discussion and recommendations

The behaviour of a cloud generated from accidental spills of SO_3 and oleum is very complicated. It will initially behave as a dense gas cloud with numerous processes occurring in it. At a certain distance downwind and after adequate dilution with air the cloud density drops and transition to passive behaviour will occur (the chemical reaction processes will cease before transition to passive behaviour occurs). The cloud generally behaves differently in the heavy and passive gas regimes. In the heavy gas regime, the

Table 5
Model sensitivity to the assumption concerning the SO_3 and H_2SO_4 relative affinity for atmospheric moisture for accidental spills of 16 kg s^{-1} for 600 s of 65% oleum (RH = 50%, U_{10} = 5 m s^{-1}) (Scenarios 5, 12, 13, 14)

Ratio of SO_3 affinity to H_2SO_4 affinity	1:1	5:1	10:1	20:1
Distance at which transition occurs (m)	410.92	349.41	349.41	349.39
Aerosol centreline concentration (mg m^{-3})				
1000 m	10.74	9.60	9.88	9.60
2500 m	1.12	1.08	1.11	1.08
5000 m	0.298	0.295	0.301	0.295
10,000 m	0.098	0.097	0.099	0.097
Settling velocity (cm s^{-1})	0.557	0.557	0.557	0.557
Deposition velocity (cm s^{-1})	0.725	0.004	0.725	0.725
Reflection coefficient	0.95	0.955	0.952	0.955

higher the wind speed or the relative humidity are, the higher the species concentration is. In the passive regime this dependence is reversed (the higher the wind speed or the relative humidity are, the lower the species concentration is). Generally the cloud behaviour is strongly affected by the wind speed, the atmospheric water content and the source strength.

It has been shown that the assumption concerning the SO_3 and H_2SO_4 vapour affinity for moisture does not affect the results. The cloud behaviour is totally different for the amount released after pool spreading has ceased. Concentrations are much lower and transition to passive behaviour occurs rapidly.

As already mentioned, the pool evolution rates in reality are not constant, but are time dependent. Furthermore, in reality the plume will not be uniform; it will have a strongly intermittent structure consisting of almost pure air with regions of more concentrated particles. Thus, a more sophisticated time dependent dispersion model could be used. Several models of this type are available. However, the use of such a model will increase the complexity of the assessment, beyond what is justified on the basis of present knowledge of processes such as aerosol nucleation, growth and deposition. In this work, attention was focused more on the thermodynamic model, as none of the available ones (even with modifications) could adequately describe these scenarios.

The main advantages of the model are:

- It describes the cloud behaviour in a more realistic way than has previously been done, taking account of all the processes that occur in it.
- Although the cloud behaviour is very complicated, calculation times are very satisfactory (e.g. less than 30 min on a Pentium 150).
- The same model can be used with slight modifications for other highly reactive species.

Unfortunately no experimental data are available. Validation and further improvement of the present model depends on the availability of these data. Therefore, it is strongly recommended that experiments should be carried out, especially to determine the following aspects:

- Aerosol nucleation and growth under high concentrations of aerosol in the atmosphere.
- Particle deposition.
- More precise kinetics on the gas phase reaction of SO_3 and H_2SO_4 with water.

8. Nomenclature

$a(x_G)$	Reflection coefficient
C_{pm}	Specific heat of the mixture in the cloud (kJ kg^{-1} K^{-1})
C	Aerosol concentration (kg m^{-3})
dx	Distance increment (m)
D_B	Brownian diffusivity (m^2 s^{-1})
f_1	Air mass mixing ratio (kg of water (kg of total air)$^{-1}$)
g	Acceleration due to gravity (m s^{-2})

h	Source height (m)
H	Plume height or depth (m)
H_r	Reference height (m)
H_s	Vertical extent or depth of the source (m)
H_s'	Vertical extent or source depth in the case of pure vapour flow (m)
H_t	Plume height at the transition point (m)
J	Nucleation rate (particles cm^{-3} s^{-1})
k	Froude number
k_i	Diffusion-limited wall loss coefficient (s^{-1})
k_1	First-order rate for the SO_3 loss (s^{-1})
k_2	Coefficient for the SO_3 loss on the ground (s^{-1})
k_3	Coefficient for the H_2SO_4 loss on the ground (s^{-1})
L	Monin–Obukov length (m)
L_1	Turbulent length scale (m)
M'	Mass rate of advection of the cloud (kg s^{-1})
M_a'	Mass rate of advection of entrainment of air per unit distance (kg s^{-1})
$M_a'(x_n)$	Mass rate of advection of the entrained air at x_n (kg s^{-1})
$M_{air}'(x_n)$	Mass rate of advection of total air present at the distance increment x_n (kg s^{-1})
$M_{air}'(x_{n-1})$	Mass rate of advection of total air present at the distance increment x_{n-1} (kg s^{-1})
$M_{aerosol}'$	Aerosol mass rate of advection (kg s^{-1})
$M_{aerosol}'(x_n)$	Mass rate of advection of aerosol present at the distance increment x_n (kg s^{-1})
$M_{aerosol}'(x_{n-1})$	Mass rate of advection of aerosol present at the distance increment x_{n-1} (kg s^{-1})
$M_{\alpha s}'$	Mass flow rate of air at the source (kg s^{-1})
$M_{H_2O,1}'$	Mass rate of water being used by the reaction of SO_3 vapour (kg s^{-1})
$M_{H_2O,2}'$	Mass rate of water being used by the reaction of H_2SO_4 vapour (kg s^{-1})
$M_{H_2SO_4}'(x_n)$	Mass rate of advection of H_2SO_4 vapour present at the distance increment x_n (kg s^{-1})
$M_{H_2SO_4}'(x_{n-1})$	Mass rate of advection of H_2SO_4 vapour present at the distance increment x_{n-1} (kg s^{-1})
$M_{SO_3}'(x_n)$	Mass rate of advection of SO_3 vapour present at the distance increment x_n (kg s^{-1})
$M_{SO_3}'(x_{n-1})$	Mass rate of advection of SO_3 vapour present at the distance increment x_{n-1} (kg s^{-1})
$M(t)'$	Vapour mass rate at the source (kg s^{-1})
MW_m	Mixture molecular weight (kg $kmol^{-1}$)
p_a	Sulphuric acid pressure (atm)
p_{ae}	Sulphuric acid equilibrium pressure (atm)
P_α	Atmospheric pressure (1 atm)
Q_{air}	Energy consumed to bring the dry air to the cloud temperature (kJ)
Q_{cond}	Energy of aerosol condensation (kJ)

$Q_{g,f}$	Forced heat convection (kJ)
$Q_{g,n}$	Natural heat convection (kJ)
Q_{H_2O}	Energy consumed to bring the water to the cloud temperature (kJ)
Q_r	Energy of reaction of SO_3 vapour with H_2O vapour (kJ)
r	Particle radius (m)
r_a	Aerodynamic resistance (m s^{-1})
r_s	Surface resistance (m s^{-1})
r_t	Transfer resistance (m s^{-1})
R_p	Pool mean radius (m)
R	Gas constant
RH	Atmospheric relative humidity (%)
Ri	Richardson number
S_a	Sulphuric acid saturation ratio
Sc	Schmidt number
SP	Atmospheric stability parameter
St	Stokes number
T_a	Air temperature (K)
T_c	Cloud temperature at x_n (K)
$T_{c,pr}$	Cloud temperature at x_{n-1} (K)
$T_g(x_n)$	Ground temperature at x_n (K)
$T_g(x_{n-1})$	Ground temperature at x_{n-1} (K)
T_m	Mean temperature used in Eq. (56) (K)
T_p	Pool mean temperature (K)
u	Wind speed at height z (m s^{-1})
u_E	Edge entrainment velocity (m s^{-1})
u_T	Top entrainment velocity (m s^{-1})
u_1	Longitudinal rms turbulent air velocity (m s^{-1})
u^*	Friction velocity of the airflow (m s^{-1})
U_f	Radial spread velocity of the cloud (m s^{-1})
U_{tr}	Translational plume velocity (m s^{-1})
U_w	Mean wind speed over height H_s (m s^{-1})
v_d	Average particles deposition velocity (m s^{-1})
v_t	Average gravitational settling velocity (m s^{-1})
W	Cloud half-width (m)
W_s	Source width (m)
W_t	Plume half-width at the transition point (m)
x	Downwind distance from the source (m)
y	Coordinate that refers to the horizontal direction
z	Coordinate that refers to the vertical direction
z_d	Reference height used in Eq. (23) (m)
z_i	Mole fractions of the vapours in the cloud
z_o	Roughness length of the substrate (m)
$[H_2O]$	Water concentration (molecule cm^{-3})
$[H_2SO_4]$	H_2SO_4 concentration (molecule cm^{-3})
$[SO_3]$	SO_3 concentration (molecule cm^{-3})

Greek letters

α	Edge mixing coefficient
α_τ	Thermal diffusivity of the mixture in the cloud ($m^2\ s^{-1}$)
α'	Constant used in Eq. (37)
$\beta 1$	First top mixing coefficient
$\beta 2$	Second top mixing coefficient
β'	Constant used in Eq. (37)
ΔH	Enthalpy difference of the cloud between successive steps (kJ)
Δ'	Fractional density excess of the cloud over air density
μ_a	Air dynamic viscosity ($kg\ s^{-1}\ m^{-1}$) ($\approx 1.8 \times 10^{-5}$)
ν	Mixture kinematic viscosity ($m^2\ s^{-1}$)
ν_a	Kinematic viscosity of air ($m^2\ s^{-1}$) ($\approx 1.5 \times 10^{-5}$)
ρ_a	Air density ($kg\ m^{-3}$)
ρ_c	Cloud density ($kg\ m^{-3}$)
ρ_p	Particle density ($kg\ m^{-3}$)
ρ_ν	Vapour density ($kg\ m^{-3}$)
σ_θ	Standard deviation of wind direction (degrees)
σ_y	Lateral standard deviation at x (degrees)
σ_{yt}	Lateral standard deviation at the transition point (degrees)
σ_z	Vertical standard deviation at x
σ_{zt}	Vertical standard deviation at the transition point (degrees)
$\sigma_{z,2R_p}$	Vertical deviation coefficient for distance equal to the pool diameter
$\sigma_z(x_G)$	Vertical standard deviation at x_G
Ψ_H	Function used in Eq. (23)

Acknowledgements

The authors wish to thank the HSE (Health and Safety Executive) and especially Mr. David Carter of the Major Hazards Assessment Unit (MHAU), for their invaluable help and for sponsoring this project (project reference numbers: RSU 3582/R75.025 and RSU 3843/R75.035).

References

[1] T. Kapias, R.F. Griffiths, A model for spills of SO_3 and oleum: Part II. Results, conclusions and discussion, J. Haz. Mat. 62 (1998) 131–142.
[2] T. Kapias, R.F. Griffiths, in: Proceedings of the 9th International Symposium on Loss Prevention and Safety Promotion in the Process Industries, Vol. 3, Spain, 1998, pp. 987–996.
[3] T. Kapias, R.F. Griffiths, in: Proceedings of the International Conference on Protection and Restoration of the Environment IV, Vol. 1, Greece, 1998, pp. 428–435.
[4] T. Kapias, R.F. Griffiths, A model for spills of SO_3 and oleum: Part I. Model description, J. Haz. Mat. 62 (1998) 101–129.
[5] G. Grint, G. Purdy, Sulphur trioxide and oleum hazard assessment, J. Loss Prev. Process Ind. 3 (1990) 117–184.

[6] R.L. Basket, P.L. Vogt, W.W. Schalk, B.M. Pobanz, ARAC Dispersion Modeling of the July 26, 1993 Oleum Tank Car Spill in Richmond, CA, EG&G Energy Measurements, Pleasanton CA, 1994.
[7] R.F. Griffiths (chairman of working party), Sulphur trioxide, oleum and sulphuric acid mist, Major Hazards Monograph, Institution of Chemical Engineers, 1996.
[8] T. Kapias, R.F. Griffiths, in: Proceedings of the 23rd NATO/CCMS International Technical Meeting on Air Pollution Modelling and Its Application, Vol. 2, Bulgaria, 1998, pp. 361–369.
[9] P.K. Raj, J.A. Morris, Source characterization and heavy gas dispersion models for reactive chemicals, technology and management systems, AFGL-TR-88-3 (I), Burlington, 1987.
[10] J.T. Jayne, U. Pöschl, Y. Chen, D. Dai, L.T. Molina, D.R. Worsnop, C.E. Kolb, M.J. Molina, Pressure and temperature dependence of the gas-phase reaction of SO_3 with H_2O and the heterogeneous reaction of SO_3 with H_2O/H_2SO_4 surfaces, J. Phys. Chem. A 101 (1997) 10000–10011.
[11] U. Pöschl, M. Canagaratna, J.T. Jayne, L.T. Molina, D.R. Worsnop, C.E. Kolb, M.J. Molina, The mass accommodation coefficient of H_2SO_4 vapor on aqueous sulfuric acid surfaces and the gaseous diffusion coefficient of H_2SO_4 in N_2/H_2O, J. Phys. Chem. A 102 (1998) 10082–10089.
[12] Kirk-Othmer's Encyclopedia of Chemical Technology, Sulfuric acid and Sulfur trioxide, 3rd edn., Vol. 22, Wiley, 1983.
[13] R. Hardman, R. Stacy, E. Dismukes, Proceedings of the U.S. Department of Energy—FETC Conference on Formation, Distribution, Impact and Fate of Sulfur Trioxide in Utility Flue Gas Streams, USA, 1998.
[14] S.F. Jagger, Development of CRUNCH: a dispersion model for continuous releases of a denser-than-air vapour into the atmosphere, UKAEA, SRD R 229, 1981.
[15] F. Pasquill, The estimation of the dispersion of windborne material, Meteorol. Mag. 90 (1063) (1961) 33–49.
[16] M. Mohan, T.S. Panwar, M.P. Singh, Development of dense gas dispersion model for emergency preparedness, Atm. Environ. 29 (16) (1994) 2075–2087.
[17] T.J. Overcamp, A general Gaussian diffusion–deposition model for elevated point sources, J. Appl. Met. 15 (1976) 1167–1171.
[18] S.R. Hanna, P.J. Drivas, Guidelines for Use of Vapor Cloud Dispersion Models, American Institute of Chemical Engineers, 1987.
[19] R.J. Taylor, J. Warner, N.E. Bacon, Scale length in atmosphere turbulence as measured from an aircraft, Quart. J.R. Met. Soc. 96 (1970) 750.
[20] R.A. Cox, R.J. Carpenter, Proceeding of a Symposium on Heavy Gas and Risk Assessment, Frankfurt, 1979, pp. 55–87.
[21] R.P. Hosker, Estimates of dry deposition and plume depletion over forests and grassland, IAEA/ST1/PUB/354, 291, 1974.
[22] B.E. Wyslouzil, J.H. Seinfeld, R.C. Flagan, Binary nucleation in acid–water systems: II. Sulfuric acid–water and a comparison with methanesulfonic acid–water, J. Chem. Phys. 94 (10) (1991) 6842–6850.
[23] J.C. Weil, Updating the ISC model through AERMIC, 85th Annual Meeting of Air and Waste Management Assoc., Kansas City, 1992.
[24] L. Post (Ed.), HGSYSTEM 3.0 Technical Reference Manual, Shell Research, 1994.
[25] R.C. Easter, L.K. Peters, Binary homogeneous nucleation: temperature and relative humidity fluctuations, nonlinearity, and aspects of new particle production in the atmosphere, J. Appl. Met. 33 (1994) 775–784.
[26] Jaecker-Voirol, P. Mirabel, Nucleation rate in a binary mixture of sulfuric acid and water vapor, J. Phys. Chem. 92 (1988) 3518–3521.
[27] G.P. Ayers, R.W. Gillet, J.L. Gras, On the vapor pressure of sulfuric acid, Atm. Environ. 15 (1980) 1221–1225.
[28] R. Steudel, Sulfuric acid from sulfur trioxide and water—a surprisingly complex reaction, Angew. Chem. Ind., Ed. Engl. 34 (12) (1995) 1313–1315.
[29] F.R. Bichowski, F.D. Rossini, Thermochemistry of Chemical Substances, 1st edn., Reinhold Publishing, New York, 1936.
[30] H.W.M. Witlox, The HEGADAS model for ground-level heavy gas dispersion: 1. Steady-state model, Atm. Environ. 28 (18) (1994) 2917–2932.
[31] J.I. Holman, Heat Transfer, 5th edn., McGraw-Hill, New York, 1981.
[32] W.H. McAdams, Heat Transmission, McGraw-Hill, New York, 1954.